AGU PUBLICATIONS

Water Resources Research

RESEARCH ARTICLE
10.1002/2016WR019903

Quantifying local rainfall dynamics and uncertain boundary conditions into a nested regional-local flood modeling system

María Bermúdez[1,2], Jeffrey C. Neal[2], Paul D. Bates[2], Gemma Coxon[2], Jim E. Freer[2], Luis Cea[1], and Jeronimo Puertas[1]

[1]Water and Environmental Engineering Group, Departamento de Métodos Matemáticos y de Representación, Universidade da Coruña, A Coruña, Spain, [2]School of Geographical Sciences, University of Bristol, Bristol, UK

Key Points:
- A method to incorporate local rainfall dynamics and inflow discharge and outflow stage uncertainty into flood predictions was developed
- A computationally efficient three-level, regional-regional-local, hydrologic-hydraulic-hydraulic model was applied and tested
- It was necessary to simulate local rainfall-runoff to capture the magnitude and timing of the flood peak stage for the selected event

Correspondence to:
M. Bermúdez,
mbermudez@udc.es

Citation:
Bermúdez, M., J. C. Neal, P. D. Bates, G. Coxon, J. E. Freer, L. Cea, and J. Puertas (2017), Quantifying local rainfall dynamics and uncertain boundary conditions into a nested regional-local flood modeling system, *Water Resour. Res.*, *53*, doi:10.1002/2016WR019903.

Received 6 OCT 2016
Accepted 4 MAR 2017
Accepted article online 7 MAR 2017

Abstract Inflow discharge and outflow stage estimates for hydraulic flood models are generally derived from river gauge data. Uncertainties in the measured inflow data and the neglect of rainfall-runoff contributions to the modeled domain downstream of the gauging locations can have a significant impact on these estimated "whole reach" inflows and consequently on flood predictions. In this study, a method to incorporate rating curve uncertainty and local rainfall-runoff dynamics into the predictions of a reach-scale flood model is proposed. The methodology is applied to the July 2007 floods of the River Severn in UK. Discharge uncertainty bounds are generated applying a nonparametric local weighted regression approach to stage-discharge measurements for two gauging stations. Measured rainfall downstream from these locations is used as input to a series of subcatchment regional hydrological model to quantify additional local inflows along the main channel. A regional simplified-physics hydraulic model is then applied to combine these contributions and generate an ensemble of discharge and water elevation time series at the boundaries of a local-scale high complexity hydraulic model. Finally, the effect of these rainfall dynamics and uncertain boundary conditions are evaluated on the local-scale model. Accurate prediction of the flood peak was obtained with the proposed method, which was only possible by resolving the additional complexity of the extreme rainfall contributions over the modeled area. The findings highlight the importance of estimating boundary condition uncertainty and local rainfall contributions for accurate prediction of river flows and inundation at regional scales.

1. Introduction

Over the last decades, flood inundation numerical models have become a powerful tool to aid flood risk management. Model sophistication has increased in line with the development of new modeling approaches, the increase of computational resources and the growing availability of remotely sensed data [*Bates*, 2004]. In the case of urban areas, inundation models can now address the topographic spatial variability and the complex floodplain connectivity caused by the presence of small-scale and geometrically complex structural elements (buildings, walls, curbs, berms, etc.). In order to do so, models of urban flooding require at least a two-dimensional treatment of the surface flow hydraulics [*Abderrezzak et al.*, 2009; *Ishigaki et al.*, 2004; *Yu and Lane*, 2006] and a high enough grid resolution to resolve the complex flow paths and local hydraulic effects [*Fewtrell et al.*, 2008; *Mark et al.*, 2004]. Two-dimensional models that solve the shallow water equations on a fine grid have thus become a well-established choice for simulating flood processes in urban environments. This approach provides predictions of the flow pattern at the scale of the individual buildings, which can serve as input for applications such as microscale flood risk analysis [*Ernst et al.*, 2010].

However, the need to represent small-scale features explicitly in the model leads to an increase of computational cost and setup requirements, which means only limited areas can be considered in practical applications. This approach is hence not suitable to simulate floodplain inundation across large spatial scales, in which case 1-D or hybrid 1-D-2-D models continue to be the most common alternative [*Bates et al.*, 2010; *De Roo et al.*, 2003; *Hunter et al.*, 2007]. Two-dimensional porous shallow water models which parameterize the effects of small-scale solid objects with a porosity parameter have also been proposed in the last years to simulate urban flood flows without the need of a very fine and computationally demanding mesh [*Cea and Vázquez-Cendón*, 2010; *Guinot*, 2012; *Schubert and Sanders*, 2012].

Regardless of the selected modeling approach, all flood inundation models require appropriate boundary conditions to be specified at the limits of the domain. Boundary conditions commonly include the upstream flow rate and the water stage at the downstream boundary of the reach being modeled. These data are usually acquired from gauging stations spaced 10–60 km apart on the river network [*Mason et al*., 2011] where water levels are measured and then converted to discharge by means of rating curves. Although generally treated as deterministic relationships, rating curves are subject to uncertainties that originate from a number of sources, such as the measuring instrument or the sampling of the cross-sectional area, which can limit their accuracy and applicability to any particular event [*Birgand et al*., 2013; *Coxon et al*., 2015; *Le Coz et al*., 2014; *McMillan et al*., 2012; *Pelletier*, 1988; *Tomkins*, 2014]. Besides, temporary hydrological conditions such as seasonal variations of the state of vegetation, changes in river geometry due to sediment dynamics, the presence of unsteady flow conditions, and the hysteresis effect add uncertainty to the derived streamflows [*Di Baldassarre et al*., 2012]. Furthermore, rating curves are seldom developed for low-frequency events and there is often a lack of stage-discharge measurements at higher flow ranges, meaning that derived streamflow records are particularly uncertain for high-return period flow estimates [*Merwade et al*., 2008]. *Mason et al*. [2011] estimate that problems with rating curve extrapolation to high flows and gauge bypassing can result in errors higher than 20% in gauged flow rates, as opposed to typically 5% in low flow conditions. *Di Baldassarre and Montanari* [2009] found that river flow records derived with the rating curve method were affected by an increasing error for increasing river discharge values, with errors in the range of 6.2–42.8% at the 95% significance level, with an average of 25.6%.

On the other hand, for fine resolution local-scale physically based models, the sparsity of the gauge network often requires flows to be routed from upstream gauge stations to the boundary of the model domain. The straightforward approach of extending the model domain up to the available gauging points involves an increase of computational burden which is not justified in practical applications. This process introduces additional uncertainty, derived not only from the flow routing method used but also from the additional lateral rainfall-runoff contributions downstream of the gauging point and before the fine-scale local model starts. This local hydrological input due to direct rainfall and/or small ungauged tributaries is generally assumed to have a minor impact on discharge in fluvial flood modeling [*Neal et al*., 2012; *Trigg et al*., 2012], but may become important in a sparse gauge network area or in flooding events with significant local rainfalls.

In those cases, a hydrological model can be used to quantify this contribution, which can subsequently be introduced as a lateral-inflow boundary condition in a hydraulic model. These lateral inflows can be formulated as point and/or uniformly distributed inflows, depending on how the hydrological and the hydraulic model are connected [*Lerat et al*., 2012]. In the simpler approaches, the lateral inflow hydrograph is estimated as a ratio of the upstream inflow [*Franchini and Lamberti*, 1994; *O'Donnell*, 1985; *Scharffenberg and Kavvas*, 2011] or is generated by a unit hydrograph rainfall-runoff model based on a design unit hydrograph known a priori [*Price*, 2009]. Alternatively, a conceptual hydrological model can be used, which is a well-established approach to simulate the rainfall-runoff transformation. The hydrological model output is also subject to a number of different sources of uncertainty including uncertainty in the input data, such as rainfall and initial moisture conditions, uncertainty in the model structure and its parameters, and uncertainty in the key model decisions such as how the model is evaluated [*Beven and Freer*, 2001; *Beven and Binley*, 1992; *Renard et al*., 2010]. The reader is referred to *Liu and Gupta* [2007] for a review of the topic of uncertainty in hydrological modeling.

In spite of the above, uncertainties in the external forcing are often overlooked and very few studies address their propagation through flood inundation models. In this sense, *Pappenberger et al*. [2006] conducted one of the few studies on the sensitivity of flood inundation predictions to uncertainty in the upstream boundary condition. The results show the uncertainty caused by the rating curve can have a significant impact on the model results, exceeding the importance of model parameter uncertainty, which has received far more attention in the literature [*Aronica et al*., 1998; *Hall et al*., 2005; *Pappenberger et al*., 2005]. Similar results are obtained by *Scharffenberg and Kavvas* [2011], who find that the uncertainty in the boundary conditions (inflow hydrograph and lateral inflow) developed for an ungauged watershed dominates the total uncertainty in the routed flood wave. The effect of uncertainty in the boundary conditions was also found to increase as the amount of lateral inflow increased in the stream. However, both studies point out that the impact depends on the hydraulic conditions in the reach, and further research is needed to

evaluate the influence of such effects in other types of hydraulic systems. In particular, the uncertainty in the downstream boundary can also be expected to have a major effect on low slope subcritical river reaches, in which backwater effects can be dominant. In these cases, the uncertainty needs to be translated into possible combinations of inflow discharge and outlet water elevation time series at the model boundaries. Nonetheless, it is not clear how this can be done in complex hydraulic systems in which, for example, tributaries may substantially affect flows in the main channel, or where gauging stations are located far from the area of interest. To the knowledge of authors, no previous study has proposed a method to generate these combinations of uncertain boundary conditions in such a system.

In this paper, a method to incorporate rating curve uncertainty and local rainfall-runoff dynamics into the predictions of a reach-scale flood inundation (hydraulic) model is proposed and applied to the July 2007 floods in Worcester, UK. The method relies on existing best-practice approaches to evaluate the importance of these two aspects in flood inundation modeling. First, the uncertainty in the rating curves is quantified and uncertainty bounds for discharge and water elevations at gauging locations are generated. Second, measured rainfall contributions downstream from the upstream gauging locations are simulated by a regional hydrological model to quantify additional inflows along the main channel. A regional simplified-physics hydraulic model is then applied to combine these inputs and generate an ensemble of both inflow discharge and outflow water elevation time series at the boundaries of a local-scale high-complexity hydraulic model. Finally, the effect of these rainfall dynamics and uncertain boundary conditions are evaluated on the local-scale model.

2. Methodology

2.1. Case Study

The flood event selected as the case study for this research took place on the lower River Severn on the 20 July 2007 and is part of a series of destructive floods that occurred in UK during that summer season. In contrast to typical winter flood events, caused by rainfall over the welsh uplands, the main rainfall contributions were over the lower basin around Worcester. On that date, exceptional rainfall totals were recorded in Gloucestershire, Worcestershire, Oxfordshire and adjacent counties covering the lower Severn basin [*Marsh and Hannaford*, 2007; *Prior and Beswick*, 2008]. As a result, peak river levels far exceeded previous maxima at several gauging stations in the region, and many rivers burst their banks [*Marsh*, 2008]. This caused widespread, severe and long-duration flooding on 20–25 July, with thousands of homes and business affected, as well as severe road and rail transport disruptions.

The area of interest for the local model is a 7 km reach in which the River Severn passes through the city of Worcester (West Midlands, England; Figure 1). This urban area lies immediately upstream the confluence of the River Teme and approximately 27 km upstream of the junction of the Severn with the River Avon. Two bridges cross the river at the city center and a weir (Diglis weir) is located at the downstream end of the studied reach. It is a low water slope, subcritical reach in which backwater effects are significant. This area corresponds to the local hydraulic model domain, which in area is toward the current reasonable upper limit for a highly resolved full shallow water model used for engineering studies. However, as is typical of many local-scale modeling studies, no upstream gauging station exists for this domain and to generate appropriate boundary conditions it is necessary to route flows from an upstream gauging station to the boundary of the local model with a simplified regional-scale routing model (Figure 1).

The regional model study area encompasses a total of 60 km of the River Severn, from the Bewdley gauge upstream to the Haw Bridge gauge downstream (Figure 1). The river has a low gradient in this reach, dropping approximately 11 m. One main tributary, the River Avon, joins the river toward the end of this reach. Bewdley gauge is the closest flow gauging station upstream of Worcester on the River Severn main stem (22 km from the local-scale model boundary) and its catchment area is 4325 km^2. Downstream, the closest flow station is Saxons Lode (17 km from the local-scale model boundary), with 6850 km^2 of catchment area. Three other significant tributaries enter the River Severn between these two gauging points: the River Stour (gauged at Kidderminster Callows Lane, with a catchment area of 324 km^2), the River Salwarpe (gauged at Harford Hill, with 184 km^2 of catchment area), and the River Teme (gauged at Knightsford Bridge, with 1480 km^2 of catchment area). These tributaries join the Severn main stem 15.5 km upstream, 1.5 km upstream, and 1 km downstream the boundaries of the local-scale model, respectively. Hence, for this

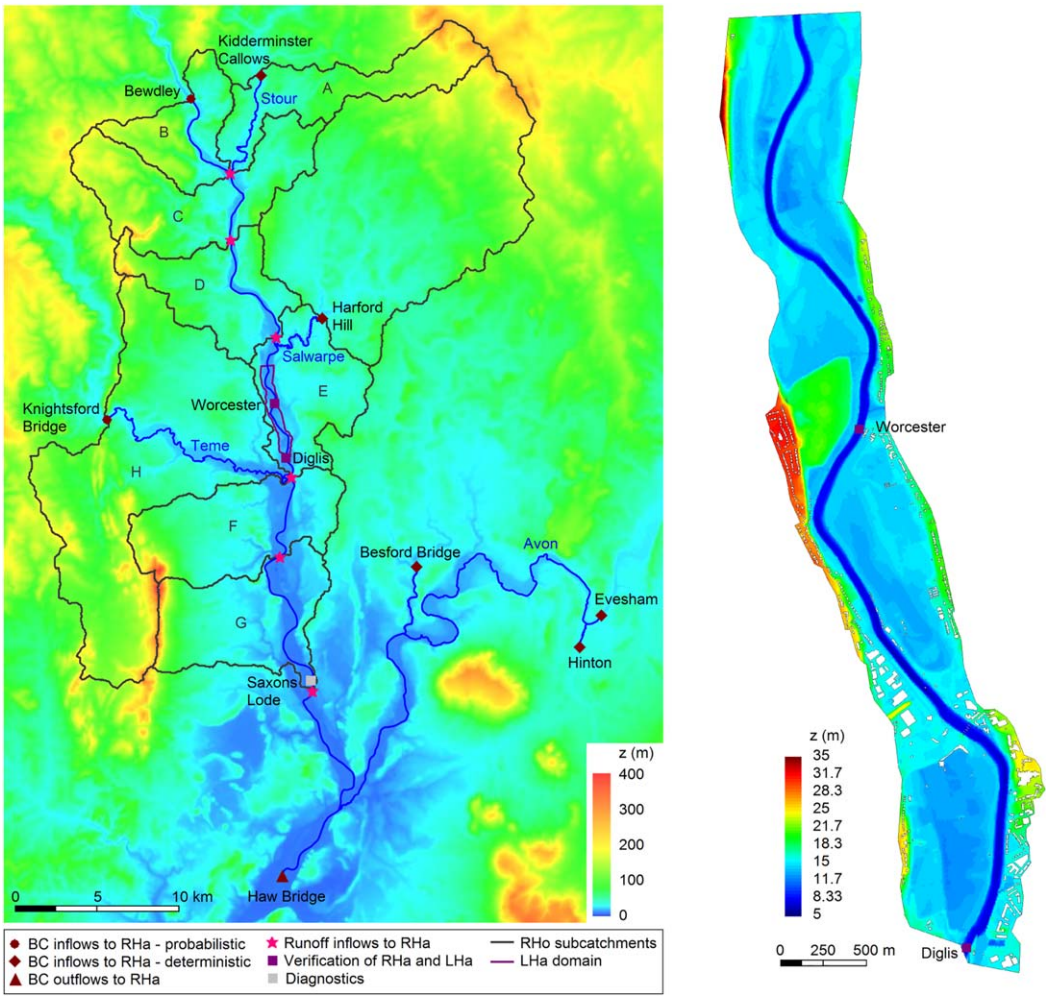

Figure 1. (left) Map showing the digital elevation model used for the regional hydraulic model (RHa), the location of gauging stations used to provide boundary condition (BC) inflows and outflows for the RHa, the subcatchment delineation (A–H) and the calibration domain (Harford Hill catchment) used in the regional hydrological model (RHo), the location of the subcatchment outlets where runoff inflows are introduced into the RHa, and the extent of the local hydraulic model (LHa) domain. (right) LHa domain with the location of gauging stations used to validate the RHa and the LHa.

domain, the catchment area between flow gauging stations extends over 537 km^2 (Figure 1). Based on the rainfall product described in *Lewis et al*. [2016], 95 mm of rainfall fell in a 24 h period over this domain during the case study event. Rainfall intensity was lower over the Bewdley catchment, reaching 64 mm in a 24 h period.

2.2. Model Configuration

The first step of the proposed methodology is the quantification of the uncertainties within the discharge records (Figure 2). The discharge uncertainty is estimated at two gauging stations: Bewdley (River Severn) and Knightsford Bridge (River Teme), based on the magnitude of the discharge and close proximity to the Worcester area (Figure 1). Given the low river slope, the contributions from the River Teme can be expected to induce backwater effects. The discharge and stage data from the remaining gauges shown in Figure 1 are treated as deterministic data. Discharge uncertainty bounds are generated applying a nonparametric local weighted regression approach to stage-discharge measurements. An error model is then used to generate an ensemble of discharge time series with heteroscedastic errors.

Due to the large local rainfall-runoff contributions for this particular flood event, the local rainfall-runoff dynamics are evaluated in the second step of the methodology (Figure 2). In order to do this, a semidistributed hydrological model comprising eight subcatchments was developed (Figure 1). Subcatchment A is the

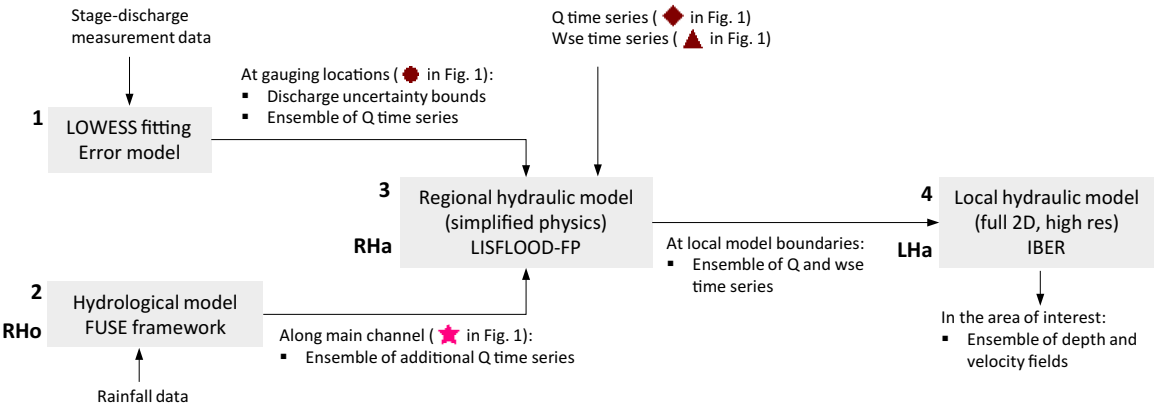

Figure 2. Flow diagram of the methodology: discharge uncertainty quantification, regional hydrologic modeling (RHo), and two-step (regional-local) hydraulic modeling cascade (RHa and LHa). To be read in conjunction with Figure 1.

River Stour, subcatchment H is the River Teme, and subcatchments B to G are the River Severn main stem. All the subcatchments areas are in the order of 50 km^2, except catchment H which was 169 km^2. This is because the outlets of the subcatchments are placed along the main channel of the Severn. Therefore, the area flowing into the River Teme is represented by a unique subcatchment, its outlet is located at the confluence of the two rivers. Hydrological models from the Framework for Understanding Structural Errors (FUSE) described in *Clark et al*. [2008] were used to simulate the rainfall-runoff process over each subcatchment. The model allows the quantification of additional inflows along the main channel, downstream from the flow gauging stations.

The third and fourth steps of the methodology correspond to the hydraulic modeling approach (Figure 2). In the nested method proposed in this paper, two different two-dimensional hydraulic models are applied consecutively: the regional-scale model LISFLOOD-FP that solves the local inertial approximation of the shallow water equations [*Bates et al*., 2010; *Neal et al*., 2015] and the local-scale model Iber that solves the full shallow water equations [*Bladé et al*., 2014; *Cea et al*., 2016]. Figure 1 shows the domains over which each model is applied. The LISFLOOD-FP model was set up to simulate a total of 60 km of the River Severn, whereas the Iber model domain covers the urban area of Worcester.

The regional hydraulic model is applied to combine the uncertainties in discharge data at gauging stations and to incorporate the local runoff inflow (Figure 2). The realizations for the discharge time series at the gauging locations are introduced as inflow boundary conditions into the regional hydraulic model. The runoff flows calculated with the hydrological model are added as point source discharges at the outlet of each subcatchment (Figure 1). The coupling between the regional hydrological model and the regional hydraulic model is executed in one way, so the runoff generation process is not affected by the surface flows calculated with the hydraulic model. Given the larger time step of the hydrological model, the runoff values are linearly interpolated to give the runoff rate at each time step of the regional hydraulic model. The runoff is specified as a source term for the hydrodynamic model.

The regional hydraulic model provides the boundary conditions for the local hydraulic model, which consist of an ensemble of inflow discharge and outflow water surface elevation time series at the upstream and downstream boundary respectively. The local-scale hydraulic model calculates the depth and velocity fields for the area of interest. It is worth noting that Diglis weir gauge is located at the downstream boundary of the local-scale model and could be used as downstream boundary condition. However, we assume this local gauge is not available, which is typical of many fine resolution modeling studies. In this way, the uncertainty of both inflows (discharge) and outflows (stage) to the local hydraulic model when close gauges are not available is considered. The local hydraulic model is one-way nested into the regional hydraulic model, so the flow of data is only from the regional model to the local model.

The use of a semidistributed hydrological model, coupled one way to the regional hydraulic model, is motivated by a compromise between a reasonably good characterization of the lateral runoff inflows and the computational efficiency needed in an uncertainty analysis framework. The alternative strategy of

simulating precipitation directly in the regional hydraulic model via a precipitation source term was discarded due to the increase in computational cost and the expected poor characterization of the overland flows given the mesh size.

On the other hand, the decision to use two different hydraulic models is driven by the need for high resolution and very accurate results in the urban area, with limited validation data available in this local domain. On the contrary, low-resolution results and simplified physics are often sufficient in the extensive area covered by the regional model, where high computational efficiency is needed. Hence, a simpler representation of the flow processes and a coarse resolution grid was selected for the regional model, whereas a full two-dimensional model and a fine resolution grid was adopted at the local scale. Overall, this nested modeling approach allows a continuous examination of the water fluxes from the catchment scale to the reach and building scale, while still requiring short setup and computational times.

2.3. Quantification of Uncertainty in Rating Curves

In the first step of the methodology, a nonparametric local weighted regression (LOWESS) approach was used to estimate discharge uncertainty from the available stage-discharge measurements at each gauging station, as explained in *Coxon et al*. [2015]. This method was chosen as it has been shown to capture place-specific discharge uncertainties for a large number of gauging stations in England and Wales. The LOWESS approach performs a weighted linear regression on a chosen span of data points around each stage-discharge measurement. The estimated variance within each span for each stage-discharge value is then calculated to quantify the uncertainty of the fit. At each point, the residual errors within the span window are assumed to be homoscedastic, independent and randomly distributed. Thus, an estimated value of discharge and variance which describes the 95% uncertainty bounds are obtained for each stage value. This method relies on the observed stage-discharge data to inform the magnitude of discharge uncertainty, which means that the methodology is unable to extrapolate beyond the limits of the gauged data and that hysteresis-induced uncertainty is not considered. We utilized the discharge uncertainty from the maximum gauged discharge point as the discharge uncertainty estimate when extrapolating beyond the stage-discharge measurements.

A first-order autoregressive model was used to generate multiple error time series for the discharge data [*Garcia-Pintado et al*., 2013]. The calculations were performed with the code developed by *Lloyd et al*. [2016]. The errors at each gauge location were assumed to be uncorrelated, as uncertainties in stage measurements and rating curves are normally independent between sites. The white noise component of the error model was scaled by a time series of standard deviations derived from the uncertainty analysis and the temporal correlation was assumed to be 5 days. This allowed for heteroscedasticity in the error over the whole range of the rating, as defined by the LOWESS results.

2.4. Evaluation of Local Rainfall-Runoff Contributions and Dynamics

In the second step of the methodology, the local rainfall-runoff dynamics were evaluated by means of a semidistributed hydrological model comprising eight subcatchments. For each subcatchment, lumped hourly measured rainfall from the product described in *Lewis et al*. [2016] and disaggregated daily Potential Evapotranspiration data from the UK Meteorological Office Rainfall and Evaporation Calculation System [*Hough and Jones*, 1997] for the year 2007 were obtained.

The flexible modeling framework, FUSE (Framework for Understanding Structural Errors) [*Clark et al*., 2008], was set up to simulate the rainfall-runoff process over each subcatchment. This framework can allow the combination of many different conceptual model choices to form hundreds of different model structures. Here we only used the four core structures from which all the different conceptual modeling choices in FUSE are based: PRMS [*Leavesley et al*., 1983], TOPMODEL [*Beven and Kirkby*, 1979], SACRAMENTO [*Burnash*, 1995], and ARNO/VIC [*Zhao*, 1984] to represent uncertainty in the hydrological model structure. Given the lack of gauging stations across the eight subcatchment areas where significant rainfall inputs occurred (see Figure 1), the best-performing model structure-parameter combinations were evaluated for the River Salwarpe catchment at the Harford Hill gauging station (Figure 1). This catchment was chosen for its proximity to the modeled area and its size, being the smallest close gauged catchment. Necessarily, we therefore assume that the best-performing models from the Monte Carlo sampling at the Harford gauge were

transferrable to the other subcatchments to quantify these additional rainfall-runoff contributions for the whole domain.

For each of the four FUSE modeling structures, we ran 10,000 Monte Carlo Sobol sequences of parameter samples for the Harford Hill gauging station for the period 1 July 2006 to 1 January 2008. The feasible parameter space for each structure was based on a previous UK study [*Coxon et al*., 2014] and was widely set to ensure they covered a range of catchment behaviors. Since the methodology is tested in hindcast mode, the measured hourly flows from the Harford Hill gauging station were compared to the model predictions using a Nash-Sutcliffe efficiency (NSE) score for the entire 2007 period. From these we obtained the best-performing models by retaining the 200 model runs that achieved the highest NSE values to capture the uncertainty in the hydrological model. These 200 structure-parameter sets were then used to quantify the within reach rainfall-runoff contributions into the flood modeling domain from each of the eight subcatchments by running these sets through FUSE driven from spatial rainfall inputs averaged for each subcatchment area.

2.5. Nested Hydraulic Modeling Approach

In the third and fourth steps of the methodology, a one-way nested hydraulic modeling approach was developed. Two hydraulic models were applied consecutively: the regional-scale model LISFLOOD-FP [*Bates et al*., 2010; *Neal et al*., 2015] and the local-scale model Iber [*Bladé et al*., 2014; *Cea et al*., 2016]. Their main features are briefly described below.

LISFLOOD-FP is a flood inundation model specifically designed to estimate floodplain inundation across large spatial scales. It solves the local inertial approximation of the shallow water equations using an explicit finite difference scheme on a Cartesian grid [*Bates et al*., 2010]. In order to run at a computationally feasible resolution at this scale, the model assumes channel flows can be represented as a subgrid-scale process, as described in *Neal et al*. [2015]. The one-dimensional local inertial wave model is used to solve the channel flows. When the water depth exceeds bankfull depth the model simulates floodplain flow, which is added to the channel flow. A free version of the model is available for download at www.bristol.ac.uk/geography/research/hydrology/models/lisflood/.

On the other hand, the local-scale model Iber solves the full depth-averaged shallow water equations in order to compute the water depth and the two horizontal components of the depth-averaged velocity. These equations are solved with an unstructured finite volume solver explicit in time, which implements the scheme of *Roe* [1986] for the discretization of the inertial terms and an upwind discretization of the topography [*Bermúdez et al*., 1998]. For a detailed description of the model, including application and validation examples, the reader is referred to *Bladé et al*. [2014] and the references therein. A free version of the model is available for download at www.iberaula.es.

The LISFLOOD-FP model was set up to simulate a total of 60 km of the River Severn (Figure 1). The locations of river channels were taken from UK Ordnance Survey mapping data and 181 ground surveyed cross sections from the Environment Agency were used to define the subgrid channel geometry. Further details on the channel shape treatment are given in *Neal et al*. [2015]. In order to define the floodplain topography, a 100 m resolution digital terrain model was created by aggregating 2 m resolution bare earth LiDAR digital elevation data from the Environment Agency. The location and parameterization of weirs in the model domain was taken from an Environment Agency 1-D model of the reach. Based on the sensitivity analysis conducted by *Neal et al*. [2015], typical physical values of 0.035 and 0.06 $s/m^{1/3}$ were selected for the Manning coefficient of the channel and the floodplain, respectively. Inflows to the model were set for the River Severn (at Bewdley), the River Stour (at Kidderminster Callows Lane), the River Salwarpe (at Harford Hill), the River Teme (at Knightsford Bridge), the River Avon (at Evesham), the Bow Brook (at Besford Bridge), and the River Isbourne (at Hinton; Figure 1). Discharge data measured at 15 min intervals are available for the aforementioned sites. Downstream levels observed at Haw Bridge gauge were prescribed as outlet boundary condition. The inflows obtained with the hydrological model were introduced into this regional hydraulic model along the main channel, at the outlet of each subcatchment (Figure 1). A 10 day spin-up period was considered in the regional hydraulic model runs, therefore the model was run from 17:30 h on 9 July to 17:30 h on 27 July 2007.

The Iber model is intended to incorporate the topographic complexity of the urban area of Worcester and to represent flows at the scale of individual buildings. Thus, the domain was discretized into an

unstructured computational mesh of approximately 200,000 triangular elements, with an average element size of 23 m^2 and a finer resolution in the urban area. The topography was defined from a 1 m resolution gridded LIDAR-based digital surface model with a vertical accuracy of ~10 cm RMSE and 42 characteristic river cross sections from a 1-D ISIS model provided by the Environmental Agency. The resulting DEM was enhanced by integrating the geometry of structures and buildings, which were extracted from a 1:1250 Ordnance Survey digital map. Both bridge piers and buildings were represented as void areas, i.e., ineffective flow areas (Figure 1). The geometry of Diglis weir was integrated into the bathymetry at the downstream end of the model domain. Typical physical values were selected for the Manning roughness coefficient, which is the only parameter of the model. It was set to 0.035, 0.09, and 0.025 $s/m^{1/3}$ in the river channel, the floodplain, and the urban area, respectively. The sensitivity of the local model to the friction parameter is low, given the model formulation (full 2-D shallow water equations) and the explicit representation of small topographic variations. Accordingly, typical values for the roughness coefficient can be expected to give a good prediction of inundation extent [*Horritt*, 2000; *Horrit and Bates*, 2002]. Boundary conditions were provided by the regional-scale LISFLOOD-FP model and consisted of discharge and water surface elevation time series at the upstream and downstream boundary respectively. A 1 day spin-up time was used, so the model was run from 17:30 h on 18 July to 17:30 h on 27 July 2007.

Although the domain is significantly smaller in the local model than in the regional one, it is still computationally more expensive to run the local model. The computation time required for each local model run is in the order of 70 h versus only 2 min for the regional model. Both times are based on standard desktop computing hardware and could be reduced with the aid of high-performance computing. If the Iber model were to be used over the entire regional domain, with an average element size double that of the local model, the computational time would be approximately tripled. Therefore, the regional-local modeling cascade selected makes the higher-physics local model more applicable and computationally feasible to run. The same applies if other commercial packages that solve the full shallow water equations are used instead of the model Iber.

In order to narrow down the number of local model runs, a sampling procedure was used. The boundary conditions obtained with the regional model were compared to each other in terms of the relative differences in discharge upstream and water level downstream at each time step. If the relative differences between two simulations were below a certain threshold value for the whole event, both upstream and downstream, only one of the two simulations was run. Each sampled run was weighted according to the number of initial runs that were removed, in order to correctly represent the distribution of the boundary condition. This sampling procedure allowed us to discard simulations with very similar external forcing.

2.6. Evaluation of Model Performance

The effect of including rainfall dynamics and uncertain boundary conditions on model performance was quantified using observed flood extent data and measured water levels. Flood extent data for this flood event were available in the form of satellite imagery. Specifically, TerraSAR-X acquired a 3 m resolution stripmap image of the region on the 25 July at 06:34 h. A flood extent map was derived from this image and was treated as a deterministic observation. This allowed the assessment of the quality of the spatial inundation prediction. The flood area index was used as a measure of fit between the observed and predicted inundation extent. This metric is defined as the ratio between the intersection of modeled and observed inundation areas and the union of modeled and observed inundation areas [*Aronica et al*., 2002; *Dung et al*., 2011].

Water surface elevation (WSE) data from the Worcester gauge station, located in the middle part of the river reach, were used to evaluate the performance of the model (Figure 1). Only stage data are available for this station. The evaluation period extended from 17:30 h on 19 July to 17:30 h on 27 July 2007 (8 days). Measured data were extracted from Environment Agency archives at a 15 min temporal resolution. The Nash-Sutcliffe model efficiency coefficient (NSE) and the root mean square error (RMSE) were selected as measures of fit and were calculated over the evaluation period.

Finally, we analyzed the model performance in terms of the timing of flood wave arrival. In order to do so, we evaluated the differences between the predicted and measured travel time of the flood wave in the regional model. We extracted the time when the maximum rate of increase in water level is reached at Bewdley gauge (T_{up}) and Diglis gauge (T_{down}) in the River Severn. The maximum rate of increase occurs at

the steepest point of the rising limb of the water level time series. We use the time difference ($T_{down} - T_{up}$) as an estimate of the travel time.

3. Results and Discussion

3.1. Discharge Uncertainty

As explained in section 2.2, the discharge uncertainty was quantified at Bewdley and Knightford Bridge gauging stations. Figure 3 shows the stage-discharge measurement data, the LOWESS fit and 95% confidence intervals. At Bewdley, relatively low discharge uncertainties were found across the flow range. There was no need to extrapolate the discharge uncertainties for this station as all flows were in bank during the flood event and there were observed stage-discharge measurements in this range (Figure 4).

At Knightsford Bridge, discharge uncertainty magnitudes had to be taken from the maximum stage-discharge measurement where the flow exceeded this value during the flood event. It is worth noting that there is additional uncertainty at this station as there are two stage-discharge measurements that were taken when the flow was out of bank. These are not captured in the discharge uncertainty analysis due to: (1) a lack of stage-discharge measurements (only two) at out of bank flows and (2) no change in the rating curve derived by local EA hydrometry team. Figure 4 shows the resulting discharge uncertainty bounds for the discharge time series generated by the error model. In total, 200 realizations for the discharge time series were obtained at each site resulting in 95% confidence discharge uncertainties of $\pm$7% and $\pm$5% for the peak flow at Bewdley and Knightsford Bridge, respectively.

3.2. Rainfall-Runoff Dynamics

A series of hydrological models were developed to simulate the local rainfall-runoff dynamics, as described in section 2.4. The results from the hydrological model of the River Salwarpe catchment (calibration catchment) show a range of NSE values above 0.8 for the year 2007 and above 0.76 considering the month of July alone. All the behavioral models correspond to the SACRAMENTO conceptual model structure [*Burnash*, 1995]. Figure 5 shows the prediction uncertainties of the hydrographs computed by the selected FUSE models constrained using data from 2007 at Harford Hill during the July 2007 flood event. It can be seen that the measured flows are well bracketed by the predicted range. The differences in predicted peak discharge between the behavioral models can reach 20 m^3/s, which represents 50% of the measured discharge value.

Once the behavioral model structure and parameter set combinations were identified, hydrological models were driven by areal-averaged rainfall inputs for the remaining eight subcatchments. Therefore, a total of 200 outflow hydrographs with hourly time steps were obtained for each subcatchment. Figure 6 shows the mean discharge time series obtained. In this figure, to make comparison easier the hydrographs have been routed downstream to Saxons Lode using a time-lag component, with flow velocity taken as 1 m/s. The higher flows correspond to subcatchment H in the River Teme, with a peak discharge of 47 m^3/s, due to its

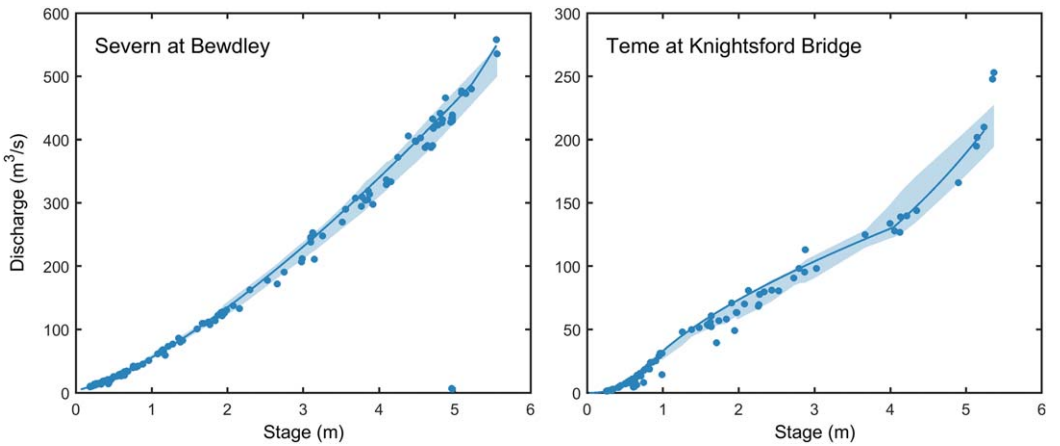

Figure 3. Stage-discharge measurements, LOWESS fit and 95% uncertainty bounds for Bewdley and Knightsford Bridge gauging stations.

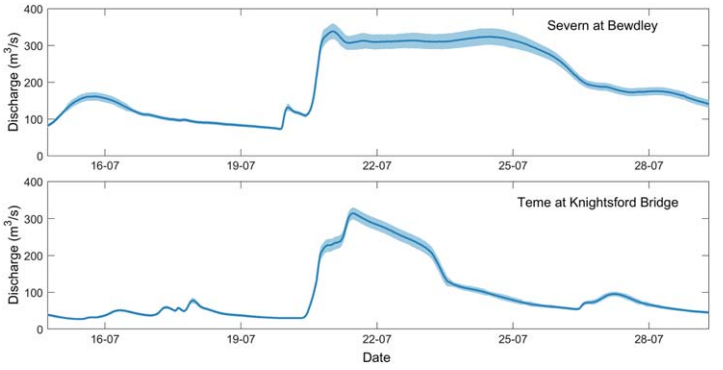

Figure 4. Discharge time series and 95th percentile uncertainty bounds at Bewdley and Knightsford Bridge gauging stations constructed using error sampling from the data in Figure 3.

larger area. For the other catchments, the average peak discharges are in the range of 7.3–17.8 m^3/s. In total, their predicted average runoff contribution at Saxons Lode reaches 131.2 m^3/s (95% confidence interval of 168.5–102.0 m^3/s). This contribution can be considered very relevant when compared with the measured peak discharge at this gauge of 545 m^3/s. It is however worth noting that the flow estimates at this gauge are known to be underestimated by up to 200 m^3/s as a result of bypass flow around the gauge at high flows (>400 m^3/s) [*Bates et al.*, 2006; *Neal et al.*, 2011].

3.3. Hydraulic Model Results and Performance

The regional hydraulic model was applied to combine the inputs from the previous two sections and generate an ensemble of discharge and water elevation time series at the boundaries of the local model. This means generating 200 realizations for the discharge time series at Bewdley, Knightsford Bridge, and the eight subcatchment outlets (Figure 1). The errors in inflows were assumed to be uncorrelated. The rest of the gauge data were treated as deterministic based on the discharge magnitude and the distance to the Worcester area. A total of 200 regional model runs are therefore run, resulting in 200 possible combinations of discharge and water time series at the upstream and downstream boundary of the local model, respectively. This would translate into an equal number of local model runs. However, a sampling procedure was used to narrow down the number of local model runs required, as explained in section 2.5. The boundary conditions of the simulations were compared with each other, in terms of relative difference in discharge upstream and water level downstream at each time step. If the relative difference between two simulations was below a certain threshold for the whole event, both upstream and downstream, only one of the two simulations is run. This allowed us to discard simulations with very similar external forcing. A relative difference threshold of 5% for discharge and 0.6% for water surface elevation was selected on the basis that the resulting envelope of the water surface elevation time series at Worcester gauge remained unchanged with additional runs. Considering the above threshold, the number of local model simulations was reduced to 30. Each of the 30 model runs was given a weighting, according to the number of initial runs with similar external forcing that were removed during the sampling procedure. This allows a correct representation of the distribution of the boundary condition (Figure 7).

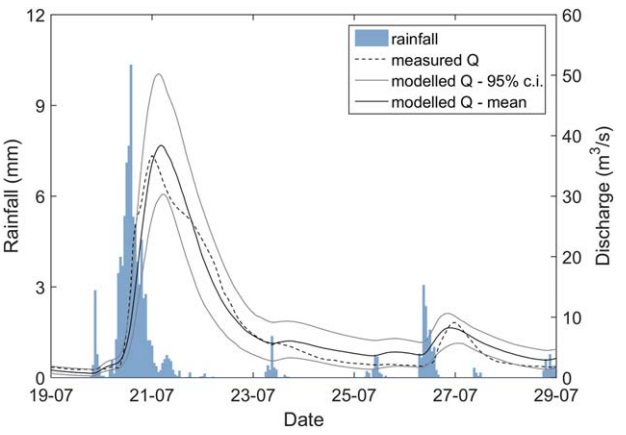

Figure 5. Mean ensemble hydrograph and 95% prediction uncertainty bounds computed by the selected FUSE models at Harford Hill, and lumped rainfall over the catchment used to drive the models. The dashed line depicts the measured discharge data.

The quality of the local model results was firstly assessed in terms of flood extent, considering the model predictions at the time of the SAR image acquisitions. A binary map of flood extent was manually derived from the SAR data and compared to the model predictions. No uncertainty in this data was taken into account due to the lack of consensus on the methods for its characterization, with few works published on this topic [*Giustarini et al.*, 2015;

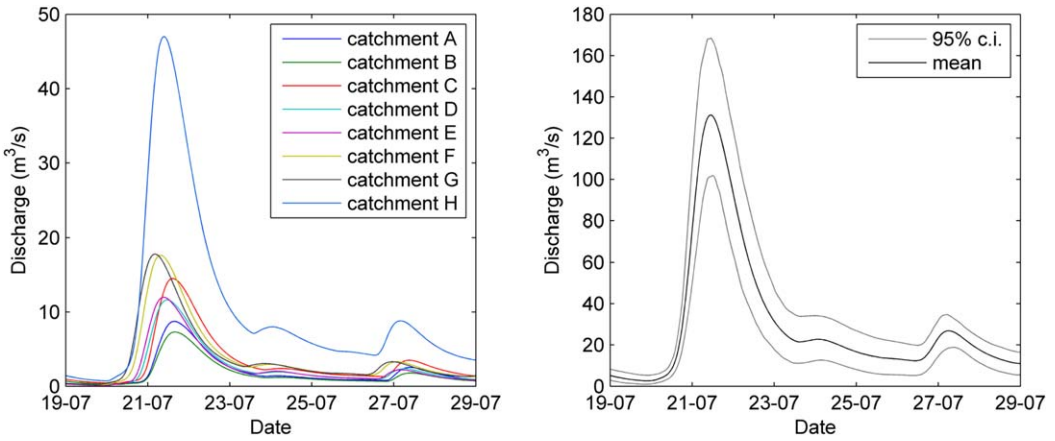

Figure 6. (left) Surface runoff contributions of each subcatchment to the streamflow at Saxons Lode based on the mean ensemble prediction values from the 200 behavioral model simulations. (right) Total predicted surface runoff contribution at Saxons Lode (mean and 95% uncertainty bounds).

Stephens et al., 2012]. The resultant flood extent prediction is in good agreement with observed data, with small differences between model runs (Figures 8 and 9). The flood area index ranges between 78 and 82%, which can be considered reasonable values given also the uncertainties in the derivation of flood extent from satellite data [*Di Baldassarre et al.*, 2009; *Schumann et al.*, 2009]. These values are toward the upper limit of flood area index values reported in previous studies which have validated fine resolution hydraulic models using SAR data [e.g., *Aronica et al.*, 2002; *Bates et al.*, 2006]. The mismatch between the observed and predicted flood extent is mainly related to model overprediction, which represents an average of 90% (standard deviation of 2.9%) of the total incorrectly predicted inundation area.

Water levels predicted by the local model at the Worcester gauge were compared to the measured values during the event. The measured water levels largely fall within the prediction interval (Figure 10). The

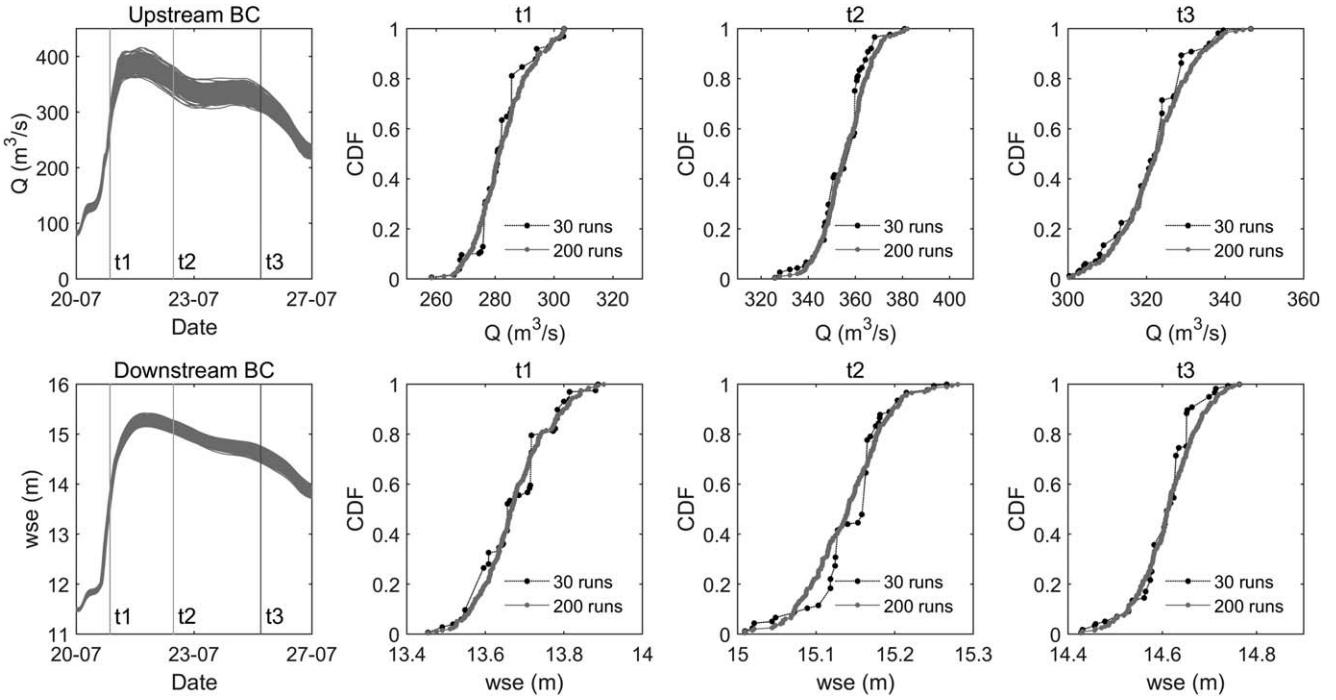

Figure 7. Discharge and water elevation time series at the boundaries of the local model obtained from the regional model (upper left and lower left figures). Cumulative distribution function (CDF) plots at different instants considering the original 200 runs and the final 30 weighted runs after sampling.

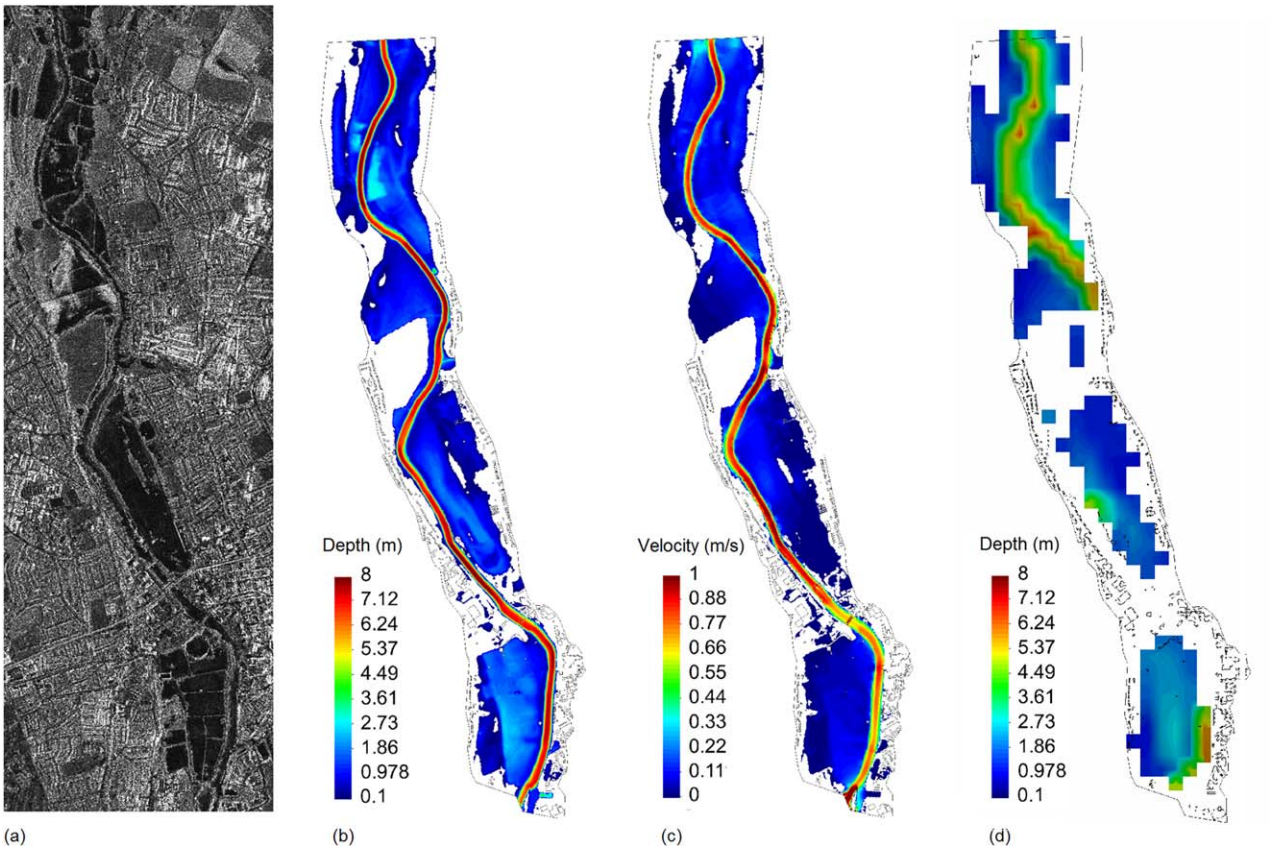

Figure 8. (a) TerraSAR-X image of Worcester flooding, example of flood depth predicted by (b) the local hydraulic model and (d) the regional hydraulic model, and (c) example of velocity field predicted by the local hydraulic model.

magnitude of the flood peak is estimated correctly, with differences below 0.30 m between the upper and lower bounds of the model runs. The model has a lower skill for predicting low flows, as can be observed at the beginning of the validation period (Figure 10). This could be attributed to the definition of weirs in the model, which are represented by a simple weir flow equation, considering a single crest elevation [*Bates et al.*, 2013]. For low flow level simulation, a more precise description of the weirs would therefore be needed. The performance of all the model runs is broadly similar, with high NSE values (between 0.92 and 0.95) and low RMSE (between 0.28 and 0.36 m).

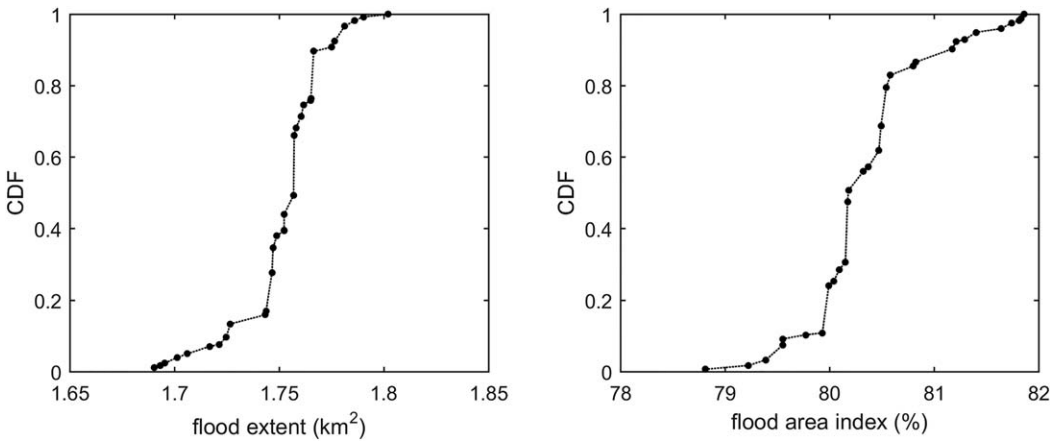

Figure 9. Cumulative distribution function (CDF) plots showing predicted flood extent (km^2) and flood area index (%) at the time of the SAR image acquisitions. Measured flood extent is 1.42 km^2.

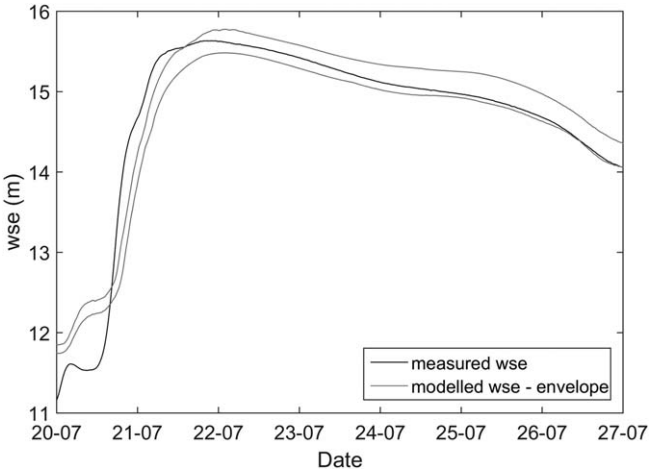

Figure 10. Predicted envelope of water surface elevation at Worcester gauge and measured values.

The main benefit of the local hydraulic model over the regional hydraulic model is the capability to produce the high-resolution accurate flow depth and velocity maps needed for detailed flood risk assessments (Figure 8). This is due to the higher mesh resolution of the local model, but also to the equations solved. Given that this case study corresponds to a subcritical flow reach, the local inertial model can be expected to compare well with the full dynamic model in terms of water surface elevations. In fact, the water levels predicted by the regional model and the local model at the Worcester gauge are very similar, and the NSE and RMSE values of the regional model runs are in the same range than those reported for the local model. However, the differences between the full dynamic model and the local inertial approximation are expected to become increasingly relevant with increasing Froude and depth gradients [*De Almeida and Bates*, 2013]. Furthermore, the local hydraulic model provides a detailed flow velocity field, especially around bridges and buildings, that cannot be determined from the regional hydraulic model.

3.4. Timing of Wave Arrival

The main discrepancy between the measured and predicted water levels lies in the timing of the peak (Figure 10). This time difference is first detected in the regional model results and is subsequently propagated into the local model from the boundary conditions. Following the procedure described in section 2.6, the calculated travel time between the upstream boundary of the River Severn (Bewdley gauge) and Diglis gauge is only 75 min, based on the measured records. In contrast, the travel time is more than tripled in the numerical results, reaching 240 min. Given that these gauging stations are 29 km apart on the River Severn, the required flood wave speed to achieve the observed 75 min wave travel time would be of 6.5 m/s, an unrealistically high value in such a low gradient system. It is therefore not possible to match the arrival time of the wave rising limb by simply decreasing the value of the Manning's coefficient or changing the channel geometry.

Figure 11 shows the water surface elevation predictions of the regional hydraulic model at the Diglis gauge, where the downstream boundary of the local model is located. It should be noted that the predicted water

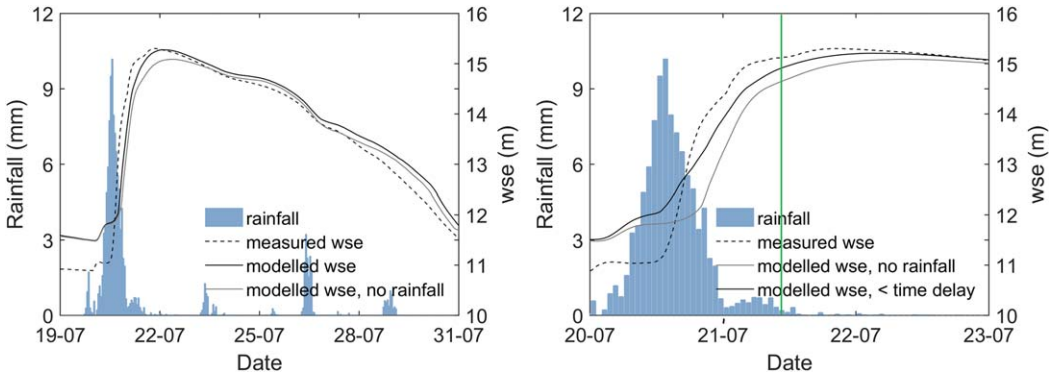

Figure 11. Comparison of measured water surface elevations at Diglis gauge and median predicted values: (1) with and without local rainfall-runoff contribution (left), (2) using the original hydrological model time delay parameter and an adjusted time delay to give an instantaneous local rainfall-runoff contribution (right). The hyetograph corresponds to the lumped hourly rainfall over the hydrological model domain. The green line represents the arrival of out of bank flows from the River Teme at this station, based on the numerical model.

level time series shown in Figure 11 is the median time series of the 200 regional model runs. The water levels predicted with different model configurations are compared to the measured values. As can be seen in Figure 11 (left), the inclusion of gauge flow uncertainty is not sufficient to achieve a good prediction of the magnitude and timing of the flood peak stage. The incorporation of the local rainfall-runoff contribution is needed to accurately predict the evolution of the water levels for this event. This is due not only to the relevant magnitude of the local runoff (please refer to section 3.2) but also to its timing. In fact, Figure 11 (left) shows how important the local rainfall-runoff contribution is to improving the prediction of both the magnitude of the flood peak and its timing. However, the improved rainfall-runoff contributed flood wave arrives only 90 min earlier, which is clearly insufficient to match the measured rising limb dynamics at Diglis exactly.

Figure 11 (right) shows the effect of adjusting the time delay parameter in the hydrological models, so that the peak of the rainfall coincides with the peak flow of the hydrographs at the subcatchment outlets. In this way, the hydrological models reproduce a nearly instant response of the catchment to the rainfall. It can be seen how the arrival of the flood wave, identified by a change of slope in the water surface elevation time series, is now better predicted. One explanation for this is the distributed nature of the rainfall-runoff process over the modeled area, which is particularly difficult to simulate using the hydrological model. In the approach proposed in this paper, model parameters are transposed from the River Salwarpe catchment at the Harford Hill gauging station (the calibration catchment) to ungauged catchments. This relies on the spatial proximity and similarity between catchments in terms of physiographic attributes and does not reflect the peculiarities in runoff forming conditions in each subcatchment. A more spatially distributed representation of the hydrological processes occurring in the model domain may therefore reproduce better this instant response and improve model performance. Besides, the uncertainty in the precipitation data used to drive the model and its hourly temporal resolution may also have an impact on runoff predictions.

However, the flood levels are still underpredicted during the rising limb with the hydrological models with adjusted time delay (Figure 11, right). This could be attributed to an underestimation of runoff volumes by the hydrological models. A better representation of the hydrological processes occurring in the model domain and the availability of more accurate input data may improve model performance. However, this could also be related to other assumptions and limitations in the rating curve uncertainty including: (1) a potential underestimation of the contributions from the River Teme for out of bank flow, (2) unaccounted hysteresis in the rating curve at Bewdley gauge in the River Severn. In the first case, the uncertainty analysis in Knightsford Bridge gauge does not capture a change in the rating curve relationship for out of bank flows, as explained in section 3.1. The methodology could be improved to include a separate treatment of the uncertainties at out of bank flow, which could result in higher predicted flows in the River Teme during this event. The flood wave from this tributary superimposes the main stem flood wave, arriving at Diglis approximately at 15:00 on 20 July. However, the arrival of out of bank flows from the River Teme at Diglis occurs after 10:00 on 21 July (green line in Figure 11, right) based on the model simulations. Therefore, the assumptions regarding uncertainty for out of bank flows do not alter the predicted timing of the wave arrival. In the second case, the analysis of direct flow measurements during this event from an ultrasonic gauge installed at Bewdley gauge showed that high flows were not significantly affected by hysteresis. Therefore, the inclusion of a loop rating curve is not expected to improve the prediction of the timing of the flood peak.

4. Conclusions

We have developed a method for incorporating the local rainfall dynamics and uncertain boundary conditions into the predictions of a reach-scale flood model. The methodology was applied to the July 2007 floods of the River Severn in the UK, considering the city of Worcester as the area of interest, with the aim of evaluating the importance of these two aspects for the hydraulic modeling of this flood event. The main conclusions that can be drawn from the results can be summarized as follows:

1. The incorporation of gauge flow uncertainty by means of existing best-practice approaches was not sufficient to achieve a good prediction of flood levels for this particular event, due to the unusual characteristics of this summer flood.

2. It was necessary to simulate local rainfall-runoff to correctly capture the flood peak stage for this event. This also significantly, but not completely, improved estimates of the timing of peak stage. Due to the distributed nature of the rainfall-runoff process, the timing was particularly difficult to simulate using a lumped semidistributed hydrological model.
3. The nested regional-local-scale model approach makes the higher-physics local model more applicable and computationally feasible to run. It provides an effective and efficient way of producing hydraulic model simulations for the common situation where a fine-scale local model is required but there is no gauge sufficiently close to the local model domain that can be reliable employed. It can be applied to flood hazard mapping in areas of high value assets, like the urban area considered in this study.
4. The proposed methodology is an efficient and tractable way for propagating boundary condition uncertainty through such nested modeling systems. The consideration of such uncertainty gives a richer view of model performance and limitations that will significantly improve confidence in the use of such modeling for decision making.

Acknowledgments
María Bermúdez gratefully acknowledges financial support from the Spanish Regional Government of Galicia (postdoctoral grant reference ED481B 2014/156-0). Gemma Coxon was supported by NERC MaRIUS: Managing the Risks, Impacts and Uncertainties of droughts and water Scarcity, grant NE/L010399/1. Jim Freer and Paul Bates by NERC Susceptibility of catchments to INTense RAinfall and flooding, grant NE/K00882X/1. A free version of the model LISFLOOD-FP is available for download at www.bristol.ac.uk/geography/research/hydrology/models/lisflood/. A free version of the model Iber is available for download at www.iberaula.es. The river cross-section data, the LiDAR digital elevation model and the gauging station rainfall, stage, flow and rating curve data of the presented case study are freely available from the Environment Agency (enquiries@environment-agency.gov.uk)

References

Abderrezzak, K. E. K., A. Paquier, and E. Mignot (2009), Modelling flash flood propagation in urban areas using a two-dimensional numerical model, *Nat. Hazards*, *50*, 433–460.
Aronica, G., B. Hankin, and K. J. Beven (1998), Uncertainty and equifinality in calibrating distributed roughness coefficients in a flood propagation model with limited data, *Adv. Water Resour.*, *22*(4), 349–365.
Aronica, G., P. D. Bates, and M. S. Horritt (2002), Assessing the uncertainty in distributed model predictions using observed binary pattern information within GLUE, *Hydrol. Processes*, *16*, 2001–2016.
Bates, P. D. (2004), Remote sensing and flood inundation modelling, *Hydrol. Processes*, *18*, 2593–2597.
Bates, P., M. Trigg, J. Neal, and A. Dabrowa (2013), *LISFLOOD-FP User Manual*, 49 pp., Univ. of Bristol, Bristol, U. K.
Bates, P. D., M. D. Wilson, M. S. Horrit, D. C. Mason, N. Holden, and A. Currie (2006), Reach scale floodplain inundation dynamics observed using airbone synthetic aperture radar imagery: Data analysis and modelling, *J. Hydrol.*, *328*, 306–318.
Bates, P. D., M. S. Horrit, and T. J. Fewtrell (2010), A simple inertial formulation of the shallow water equations for efficient two-dimensional flood inundation modelling, *J. Hydrol.*, *387*, 33–45.
Bermúdez, A., A. Dervieux, J. A. Desideri, and M. E. Vázquez-Cendón (1998), Upwind schemes for the two-dimensional shallow water equations with variable depth using unstructured meshes, *Comput. Methods Appl. Mech. Eng.*, *155*, 49–72.
Beven, K. J., and A. Binley (1992), The future of distributed models—Model calibration and uncertainty prediction, *Hydrol. Processes*, *6*(3), 279–298.
Beven, K. J., and J. Freer (2001), Equifinality, data assimilation, and uncertainty estimation in mechanistic modelling of complex environmental systems using the GLUE methodology, *J. Hydrol.*, *249*(1-4), 11–29.
Beven, K. J., and M. J. Kirkby (1979), A physically based, variable contributing area model of basin hydrology, *Hydrol. Sci. Bull.*, *24*, 43–69.
Birgand, F., G. Lellouche, and T. W. Appelboom (2013), Measuring flow in non-ideal conditions for short-term projects: Uncertainties associated with the use of stage-discharge rating curves, *J. Hydrol.*, *503*, 186–195.
Bladé, E., L. Cea, G. Corestein, E. Escolano, J. Puertas, M. E. Vázquez-Cendón, J. Dolz, and A. Coll (2014), Iber: Herramienta de simulación numérica del flujo en ríos, *Rev. Int. Métodos Numér. Cálculo Diseño Ing.*, *30*(1), 1–10.
Burnash, R. J. C. (1995), The NWS River Forecast System-Catchment modeling, in *Computer Models of Watershed Hydrology*, edited by V. P. Singh, pp. 311–366, Water Resour. Publ., Littleton, Colo.
Cea, L., and M. E. Vázquez-Cendón (2010), Unstructured finite volume discretization of two-dimensional depth-averaged shallow water equations with porosity, *Int. J. Numer. Methods Fluid*, *63*, 903–930.
Cea, L., M. Bermudez, J. Puertas, E. Blade, G. Corestein, E. Escolano, A. Conde, B. Bockelmann-Evans, and R. Ahmadian (2016), IberWQ: New simulation tool for 2D water quality modelling in rivers and shallow estuaries, *J. Hydroinf.*, *18*(5), 816–830, doi:10.2166/hydro.2016.235.
Clark, M. P., A. G. Slater, D. E. Rupp, R. A. Woods, J. A. Vrugt, H. V. Gupta, T. Wagener, and L. E. Hay (2008), Framework for Understanding Structural Errors (FUSE): A modular framework to diagnose differences between hydrological models, *Water Resour. Res.*, *44*, W00B02, doi:10.1029/2007WR006735.
Coxon, G., J. Freer, T. Wagener, N. A. Odoni, and M. Clark (2014), Diagnostic evaluation of multiple hypotheses of hydrological behaviour in a limits-of-acceptability framework for 24 UK catchments, *Hydrol. Processes*, *28*, 6135–6150.
Coxon, G., J. Freer, I. K. Westerberg, T. Wagener, R. Woods, and P. J. Smith (2015), A novel framework for discharge uncertainty quantification applied to 500 UK gauging stations, *Water Resour. Res.*, *51*, 5531–5546, doi:10.1002/2014WR016532.
De Almeida, G. A. M., and P. Bates (2013), Applicability of the local inertial approximation of the shallow water equations to flood modeling, *Water Resour. Res.*, *49*, 4833–4844, doi:10.1002/wrcr.20366.
De Roo, A. P. J., et al. (2003), Development of a European flood forecasting system, *Int. J. River Basin Manage.*, *1*(1), 49–59.
Di Baldassarre, G., and A. Montanari (2009), Uncertainty in river discharge observations: A quantitative analysis, *Hydrol. Earth Syst. Sci.*, *13*, 913–921, doi:10.5194/hess-13-913-2009.
Di Baldassarre, G., G. Schumann, and P. D. Bates (2009), A technique for the calibration of hydraulic models using uncertain satellite observations of flood extent, *J. Hydrol.*, *367*, 276–282.
Di Baldassarre, G., F. Laio, and A. Montanari (2012), Effect of observation errors on the uncertainty of design floods, *Phys. Chem. Earth*, *42-44*, 85–90.
Dung, N. V., B. Merz, A. Bárdossy, T. D. Thang, and H. Apel (2011), Multi-objective automatic calibration of hydrodynamic models utilizing inundation maps and gauge data, *Hydrol. Earth Syst. Sci.*, *15*, 1339–1354, doi:10.5194/hess-15-1339-2011.
Ernst, J., B. J. Dewals, S. Detrembleur, P. Archambeau, S. Erpicum, and M. Pirotton (2010), Micro-scale flood risk analysis based on detailed 2D hydraulic modelling and high resolution geographic data, *Nat. Hazards*, *55*(2), 181–209.
Fewtrell, T. J., P. D. Bates, M. Horritt, and N. M. Hunter (2008), Evaluating the effect of scale in flood inundation modelling in urban environments, *Hydrol. Processes*, *22*, 5107–5118.
Franchini, M., and P. Lamberti (1994), A flood routing Muskingum type simulation and forecasting model based on level data alone, *Water Resour. Res.*, *30*(7), 2183–2196.

Garcia-Pintado, J., J. C. Neal, D. C. Mason, S. L. Dance, and P. D. Bates (2013), Scheduling satellite-based SAR acquisition for sequential assimilation of water level observations into flood modelling, *J. Hydrol.*, *495*, 252–266, doi:10.1016/j.jhydrol.2013.03.050.
Giustarini, L., H. Vernieuwe, J. Verwaeren, M. Chini, R. Hostache, P. Matgen, N. E. C. Verhoest, and B. De Baets (2015), Accounting for image uncertainty in SAR-based flood mapping, *Int. J. Appl. Earth Obs. Geoinf.*, *34*, 70–77.
Guinot, V. (2012), Multiple porosity shallow water models for macroscopic modelling of urban floods, *Adv. Water Resour.*, *37*, 40–72.
Hall, J., S. Tarantolo, P. Bates, and M. S. Horritt (2005), Distributed sensitivity analysis of flood inundation model calibration, *J. Hydraul. Eng.*, *131*(2), 117–126.
Horritt, M. S. (2000), Calibration and validation of a 2-dimensional finite element flood flow model using satellite radar imagery, *Water Resour. Res.*, *36*(11), 3279–3291.
Horrit, M. S., and P. D. Bates (2002), Evaluation of 1D and 2D numerical models for predicting river flood inundation, *J. Hydrol.*, *268*, 87–99.
Hough, M., and R. J. A. Jones (1997), The United Kingdom Meteorological Office rainfall and evaporation calculation system: MORECS version 2.0—An overview, *Hydrol. Earth Syst. Sci.*, *1*(2), 227–239.
Hunter, N. M., P. D. Bates, M. S. Horritt, and M. D. Wilson (2007), Simple spatially-distributed models for predicting flood inundation: A review, *Geomorphology*, *90*(3-4), 208–225.
Ishigaki, T., H. Nakagawa, and Y. Baba (2004), Hydraulic model test and calculation of flood in urban area with underground space, in *Proceedings of the 4th International Symposium on Environmental Hydraulics and 14th Congress of Asia and Pacific Division, International Association of Hydraulic Engineering and Research, 15-18 December 2004*, edited by J. H. W. Lee and K. M. Lam, pp. 1411–1416, CRC Press, Hong Kong.
Leavesley, G. H., R. W. Lichty, B. M. Troutman, and L. G. Saindon (1983), Precipitation-runoff modeling system: User's manual, *U.S. Geol. Surv. Water Invest. Rep.*, 83-4238, 207 pp.
Le Coz, J., B. Renard, L. Bonnifait, F. Branger, and R. Le Boursicaud (2014), Combining hydraulic knowledge and uncertain gaugings in the estimation of hydrometric rating curves: A Bayesian approach, *J. Hydrol.*, *509*, 573–587.
Lerat, J., C. Perrin, V. Andréassian, C. Loumagne, and P. Ribstein (2012), Towards robust methods to couple lumped rainfall-runoff models and hydraulic models: A sensitivity analysis on the Illinois River, *J. Hydrol.*, *418-419*, 123–135.
Lewis, E., S. Blenkinsop, N. Quinn, J. Freer, G. Coxon, R. Woods, P. Bates, and H. Fowler (2016), A gridded hourly rainfall dataset for the UK applied to a national physically-based modelling system, Geophys. Res. Abstr., 18, EGU 2016-14348.
Liu, Y., and H. V. Gupta (2007), Uncertainty in hydrologic modeling: Toward an integrated data assimilation framework, *Water Resour. Res.*, *43*, W07401, doi:10.1029/2006WR005756.
Lloyd, C. E. M., J. E. Freer, P. J. Johnes, G. Coxon, and A. L. Collins (2016), Discharge and uncertainty: Implications for nutrient flux estimation in small streams, *Hydrol. Processes*, *30*, 135–152.
Mark, O., S. Weesakul, C. Apirumanekul, S. B. Aroonnet, and S. Djordjevic (2004), Potential and limitations of 1D modelling of urban flooding, *J. Hydrol.*, *299*(3-4), 284–299.
Marsh, T. (2008), A hydrological overview of the summer 2007 floods in England and Wales, *Weather*, *63*(9), 274–279.
Marsh, T. J., and J. Hannaford (2007), The Summer 2007 Floods in England and Wales—A Hydrological Appraisal, Cent. for Ecol. and Hydrol., Wallingford, Conn.
Mason, D. C., G. J-P. Schumann, and P. D. Bates (2011), Data utilization in flood inundation modelling, in *Flood Risk Science and Management*, edited by G. Pender and H. Faulkner, pp. 211–233, Wiley-Blackwell, Chichester, U. K.
McMillan, H., T. Krueger, and J. Freer (2012), Benchmarking observational uncertainties for hydrology: Rainfall, river discharge and water quality, *Hydrol. Processes*, *26*(26), 4078–4111.
Merwade, V., F. Olivera, M. Arabi, and S. Edleman (2008), Uncertainty in flood inundation mapping—Current issues and future directions, *J. Hydraul. Eng.*, *13*(7), 608–620.
Neal, J., G. Schuman, T. Fewtrell, M. Budimir, P. Bates, and D. Mason (2011), Evaluating a new LISFLOOD-FP formulation with data from the summer 2007 floods in Tewkesbury, UK, *J. Flood Risk Manage.*, *4*, 88–95.
Neal, J., G. Schumann, and P. Bates (2012), A subgrid channel model for simulating river hydraulics and floodplain inundation over large and data sparse areas, *Water Resour. Res.*, *48*, W11506, doi:10.1029/2012WR012514.
Neal, J. C., N. A. Odoni, M. A. Trigg, J. E. Freer, J. Garcia-Pintado, D. C. Mason, M. Wood, and P. Bates (2015), Efficient incorporation of channel cross-section geometry uncertainty into regional and global scale flood inundation models, *J. Hydrol.*, *529*, 169–183.
O'Donnell, T. (1985), A direct three-parameter Muskingum procedure incorporating lateral inflow, *J. Hydrol. Sci.*, *30*(4), 479–496.
Pappenberger, F., K. Beven, M. Horritt, and S. Blazkova (2005), Uncertainty in the calibration of effective roughness parameters in HEC-RAS using inundation and downstream level observations, *J. Hydrol.*, *302*, 46–69.
Pappenberger, F., P. Matgen, K. J. Beven, J. B. Henry, L. Pfister, and P. De Fraipont (2006), Influence of uncertain boundary conditions and model structure on flood inundation predictions, *Adv. Water Resour.*, *29*, 1430–1449.
Pelletier, P. M. (1988), Uncertainties in the single determination of river discharge: A literature review, *Can. J. Civ. Eng. News*, *15*(5), 834–850.
Price, R. K. (2009), An optimized routing model for flood forecasting, *Water Resour. Res.*, *45*, W02426, doi:10.1029/2008WR007103.
Prior, J., and M. Beswick (2008), The exceptional rainfall of 20 July 2007, *Weather*, *63*(9), 261–267.
Renard, B., D. Kavetski, G. Kuczera, M. Thyer, and S. W. Franks (2010), Understanding predictive uncertainty in hydrologic modeling: The challenge of identifying input and structural errors, *Water Resour. Res.*, *46*, W05521, doi:10.1029/2009WR008328.
Roe, P. L. (1986), A basis for the upwind differencing of the two-dimensional unsteady Euler equations, *Numer. Methods Fluid Dyn.*, *2*, 55–80.
Scharffenberg, W. A., and M. L. Kavvas (2011), Uncertainty in flood wave routing in a lateral-inflow-dominated stream, *J. Hydraul. Eng.*, *16*(2), 165–175.
Schubert, J. E., and B. F. Sanders (2012), Building treatments for urban flood inundation models and implications for predictive skill and modeling efficiency, *Adv. Water Resour.*, *41*, 49–64.
Schumann, G., P. D. Bates, M. S. Horrit, P. Matgen, and F. Pappenberger (2009), Progress in integration of remote sensing–derived flood extent and stage data and hydraulic models, *Rev. Geophys.*, *47*, RG4001, doi:10.1029/2008RG000274.
Stephens, E. M., P. D. Bates, J. E. Freer, and D. C. Mason (2012), The impact of uncertainty in satellite data on the assessment of flood inundation models, *J. Hydrol.*, *414-415*, 162–173.
Tomkins, K. M. (2014), Uncertainty in streamflow rating curves: Methods, controls and consequences, *Hydrol. Processes*, *28*(3), 464–481.
Trigg, M. A., P. D. Bates, M. D. Wilson, G. Schumann, and C. Baugh (2012), Floodplain channel morphology and networks of the middle Amazon River, *Water Resour. Res.*, *48*, W10504, doi:10.1029/2012WR011888.
Yu, D., and S. N. Lane (2006), Urban fluvial flood modelling using a two-dimensional diffusion-wave treatment, part 1: Mesh resolution effects, *Hydrol. Processes*, *20*(7), 1541–1565.
Zhao, R. J. (1984), *Watershed Hydrological Modelling [in Chinese]*, Chin. Water Conserv. and Electr. Power Press, Beijing.